Peak-to-Average Power Ratio Reduction Using *N*-tuple Selective Mapping Method for MC-CDMA

Sajjad Ali, Zhe Chen, and Fuliang Yin

The multi-carrier transmission signal in Multi-Carrier Code Division Multiple Access (MC-CDMA) has a high peak-to-average power ratio (PAPR), which results in nonlinear distortion and deteriorative system performance. An *n*-tuple selective mapping method is proposed to reduce the PAPR, in this paper. This method generates 2^n sequences of an original data sequence by adding *n*-tuple of *n* PAPR control bits to it followed by an interleaver and error-control code (ECC) to reduce its PAPR. The convolutional, Golay, and Hamming codes are used as ECCs in the proposed scheme. The proposed method uses different numbers of the *n* PAPR control bits to accomplish a noteworthy PAPR reduction and also avoids the need for a side-information transmission. The simulation results authenticate the effectiveness of the proposed method.

Keywords: MC-CDMA, peak-to-average power ratio, PAPR, high power amplifier, HPA, selective mapping, SLM.

Sajjad Ali (corresponding author, sajjad.ali@mail.dlut.edu.cn), Zhe Chen (zhechen@dlut.edu.cn), and Fuliang Yin (flyin@dlut.edu.cn) are with the School of Information and Communication Engineering, Dalian University of Technology, China.

I. Introduction

A Multi-Carrier Code Division Multiple Access (MC-CDMA) system, also known as an orthogonal frequency-division multiplexing (OFDM) code division multiple access (CDMA) system, is a transmission technique proffering many alluring properties, such as high spectral efficiency and low receiver complexity, which makes it a promising candidate for next-generation mobile radio systems [1]. In the MC-CDMA scheme, orthogonal codes are used to spread the symbols of users and to combine them in the frequency domain; this results in a relatively low symbol rate and non-selective fading in each subcarrier [2]. However, a severe disadvantage of multi-carrier transmission schemes, including the MC-CDMA, is the high peak-to-average power ratio (PAPR) [3]–[6]. A high PAPR at the high power amplifier (HPA) may result in in-band distortion, which degrades the bit error rate (BER), and out-of-band radiation, which interferes with adjacent frequency bands. To avoid both the in-band distortion and the out-of-band radiation, the nonlinear amplifier needs to operate close to the linear region, which results in a significant power-efficiency penalty and makes the transmitters very expensive and impractical for low-cost applications [7]–[10].

A number of PAPR reduction methods have been proposed and implemented [11]. One straightforward method is to premeditatedly clip the multi-carrier (MC) transmission signal before amplification [12]. Clipping can improve the PAPR performance, but this is a nonlinear process that may cause momentous in-band distortion, which deteriorates the BER performance, and out-of-band noise, which decreases the spectral efficiency [11]. There are also other distortionless methods, such as partial transmit sequences (PTS) [13] and selective mapping (SLM) [14]–[15]. The PTS method tries to

find an optimal combination of phase-rotated signal sub-blocks to minimize the peak power of the transmitted signal, while in the SLM method, the frequency-domain data is multiplied by a set of statistically independent sequences, and the corresponding time-domain signal with the smallest PAPR is selected and transmitted. Both methods provide improved PAPR performance but need the side information to recover the original MC signal in the receiver [11]. Although these methods were originally proposed for the OFDM system, they can, with minor modifications, be implemented in an MC-CDMA system [16]–[19]. Moreover, the SLM method is more effective in reducing the PAPR than the PTS method, for the same amount of side information. This is because in the PTS the phase must be rotated by clusters, whereas in the SLM method, the phase is rotated only by one subcarrier. Thus, there is a higher probability of achieving a low PAPR under the SLM method, as opposed to under the PTS method [17], [20].

In [17]–[19], the SLM method was used to reduce the PAPR for an MC-CDMA scheme. In [17], different phase sequences were examined, and simulation results showed that using the SLM method with a random phase sequence is most effective in reducing the PAPR. In [18], the SLM method along with selected spread code is used, where the Walsh–Hadamard transform (WHT) is employed as the phase sequence and Walsh–Hadamard codes as the spreading code. In the code selection process, the transmitter selects the spreading code of each user from a set of Walsh–Hadamard codes, and the code that provides the smallest PAPR after the application of an inverse discrete Fourier transform (IDFT) will be assigned to each user to minimize the output peak power in each symbol. In [19], a new pseudorandom interferometry code sequence was used as the phase sequence for the SLM method to reduce the PAPR in an MC-CDMA scheme.

In [14]–[15] and [17]–[19], the SLM method was used either with different phase sequences or with a spreading-code selection algorithm, but in all cases, the various methods were required to send side information, relating to either the phase sequence or the spreading code, to the receiver.

In this paper, an improved SLM method with n-tuple of n PAPR control bits followed by an interleaver and error-control code (ECC) is proposed for the reduction of PAPR in an MC-CDMA scheme. The n-tuple SLM (NTSLM) method generates 2^n data sequences of an original data sequence by adding n-tuple of n PAPR control bits to it followed by an interleaver and ECC. The use of the interleaver and ECC makes each sequence more random and reduces the probability of in-phase addition of subcarriers, which in turn, increases the probability of PAPR reduction. The convolutional, Golay, and Hamming codes are used as the ECCs in this paper. The use of

ECCs benefits the NTSLM method in terms of the error-correction capability at the receiver, which in turn, aids in the reduction of PAPR and in avoiding the need to transmit side information to recover the original data sequence at the receiver. The NTSLM uses anywhere between two to seven of the n PAPR control bits to show the flexibility and effectiveness of the proposed method.

The rest of this paper is organized as follows. The system model for the MC-CDMA scheme and PAPR statistics are presented in Section II. The need to reduce the PAPR is discussed in Section III. In Section IV, the proposed method, NTSLM, ECCs, and computational complexity are discussed. A discussion of the simulations and results are presented in Section V, and finally, some conclusions are drawn in Section VI.

II. PAPR of MC-CDMA Signal

MC-CDMA is an MC transmission scheme in which the original data payload is first multiplied with the spreading sequence, and then the chips of the spread data are modulated onto orthogonal subcarriers [1]. Figure 1 shows an MC-CDMA signal generation of a complex data symbol, $a^{(h)}$, assigned to user h. In the transmitter of Fig. 1, data symbol $a^{(h)}$ is first multiplied with a user-specific spread code, $\mathbf{b}^{(h)} = [b_0^{(h)}, b_1^{(h)}, \dots, b_{D-1}^{(h)}]^{\mathrm{T}}$, of a spread factor, D. The spread data sequence, $\mathbf{c}^{(h)}$, obtained after spreading, can be given in vector notation as $\mathbf{c}^{(h)} = a^{(h)}\mathbf{b}^{(h)} = [c_0^{(h)}, c_1^{(h)}, \dots, c_{D-1}^{(h)}]^{\mathrm{T}}$. The spread sequence $\mathbf{c}^{(h)}$ is converted to parallel $C_d^{(h)}(d = 0, \dots, D-1)$ and modulated onto $N = 1 \times D$ subcarriers followed by an IDFT of size $N_{\mathrm{IDFT}} = N$ to obtain an MC spread spectrum signal. A time-domain baseband transmission signal $x^{(h)}(t)$, after an IDFT, for one MC-CDMA symbol, $0 \le t \le T_s$, is

$$x^{(h)}(t) = \sum_{d=1}^{D} \sum_{h=1}^{H} a^{(h)} \mathbf{b}_d^{(h)} e^{2\pi j t(d-1)/T_s}, \qquad (1)$$

where T_s is the MC-CDMA symbol period, t is time, and H is the total number of users.

The PAPR for the MC-CDMA baseband signal in (1) is defined as the ratio of the maximum instantaneous peak power
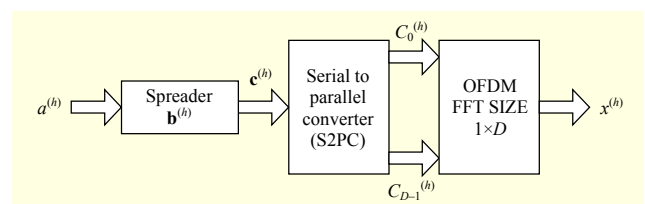

Fig. 1. MC-CDMA signal generation.

to the average power of the MC-CDMA signal [1], [8] and is given as follows:

$$\text{PAPR} = \frac{\max |x(t)|^2}{P_{\text{av}}}, \qquad (2)$$

where P_{av} is the average power, which can be calculated as

$$P_{\text{av}} = \frac{1}{T_S} \int_0^{T_S} |x(t)|^2 \, dt = \frac{1}{N} \sum_{n=0}^{N-1} \text{E}\left(\left| \sum_{h=1}^{H} x^{(h)}(n) \right|^2 \right), \qquad (3)$$

where N is the number of subcarriers. Correspondingly, PAPR in a discrete time-domain can be expressed as

$$\text{PAPR} = \frac{\max \left(|x(n)|^2 \right)}{\frac{1}{N} \sum_{n=0}^{N} \text{E}\left(|x(n)|^2 \right)}, \qquad (4)$$

where $\text{E}(\bullet)$ is the mathematical expectation operator.

Since the user data are random in nature, it is necessary to evaluate the statistical characteristics of the PAPR. The most classical approach for the analyses of PAPR is to use the complementary cumulative distribution function (CCDF), which is described as the probability of the PAPR exceeding a certain level, w [21]; that is,

$$\text{CCDF(PAPR)} = \text{prob}\{\text{PAPR} > w\} = 1 - (1 - e^{-w})^N. \qquad (5)$$

III. Need to Reduce PAPR

An MC-CDMA baseband signal is the superposition of many independent signals modulated onto subchannels. When the samples from all the subcarriers are in phase, the peak power of the signal becomes N times that of the average power; that is, PAPR = 10 log(N). Thus, this results in high PAPR. A typical MC transmission system uses an HPA to produce an output transmit power that is a multiple of the input transmit power, which has a limited linear region. Figure 2 presents a typical power characteristic of HPA. Thus, MC transmission signals with a PAPR that is larger than the saturation point of the HPA will be clipped, resulting in deteriorations in both spectrum efficiency and energy efficiency [3]. To avoid this nonlinear distortion, either the linear range of HPA should be increased; that is, the value of input back off (IBO) should be greater than the PAPR, or the PAPR should be kept smaller than the IBO value. However, the power consumption of HPA increases as the value of IBO increases, which leads to an inefficient HPA and results in expensive transmitters. Therefore, the best option, to improve energy efficiency and spectrum efficiency of MC transmission systems, is PAPR reduction techniques. Thus, there is a strong need to optimize the PAPR reduction for an energy-efficient HPA.
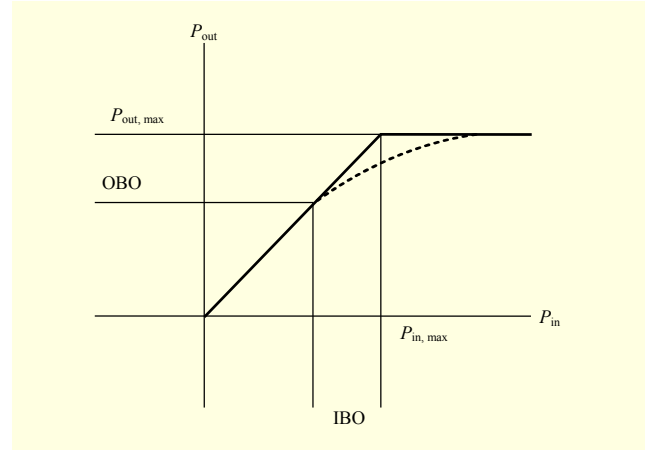

Fig. 2. Typical power characteristics of HPA.

IV. N-tuple NTSLM Method

An NTSLM method that uses n-tuple of n PAPR control bits followed by an interleaver and ECC is presented in this section. This new approach uses the same principle for improved PAPR reduction as in the SLM method [8], but in addition to this, it has the added bonus of an error-correction capability, as it employs ECCs, and avoids the need to transmit side information. A block diagram of an MC-CDMA transmitter using the NTSLM method is shown in Fig. 3(a).

In the NTSM method, n-tuple of n PAPR control bits are added to the spread data sequence $\mathbf{c}^{(h)}$ to generate 2^n spread data sequences, represented as $\mathbf{U} = [U_0, U_1, \dots, U_{2^n-1}]$, where

$$U_0 = [000000\mathbf{c}^{(h)}]$$
$$U_1 = [000001\mathbf{c}^{(h)}]$$
$$\vdots \qquad\qquad (6)$$
$$U_{2^n-1} = [111111\mathbf{c}^{(h)}].$$

These 2^n spread data sequences are statistically independent sequences. After that, $\mathbf{U}$ spread data sequences are passed through an interleaver. An interleaver is a device that operates on a block of O symbols and permutes them; thus, a data block, $\mathbf{V} = [V_0, V_1, \dots, V_{O-1}]^T$, becomes $\mathbf{V}' = [V_{\pi(0)}, V_{\pi(1)}, \dots, V_{\pi(O-1)}]^T$, where $\{o\} \leftrightarrow \{\pi(o)\}$ is a one-to-one mapping and $\pi(o) \in \{0, 1, \dots, O-1\}$ for all o. To interleave $\mathbf{U}$ spread data sequences, $\mathbf{U}$ interleaves are used to produce $\mathbf{Y}$ permuted spread data sequences, represented as $\mathbf{Y} = [Y_0, Y_1, \dots, Y_{2^n-1}]$. The permutation indices $\{\pi(o)\}$ are stored in the memory of both the transmitter and the receiver; thus, interleaving and deinterleaving can be done simply.

After interleaving, $\mathbf{Y}$ permuted spread data sequences are fetched to error-control coding. In this paper, Hamming, Golay, and convolutional ECCs are used, each of which is described in detail in the next section. The output from error-control
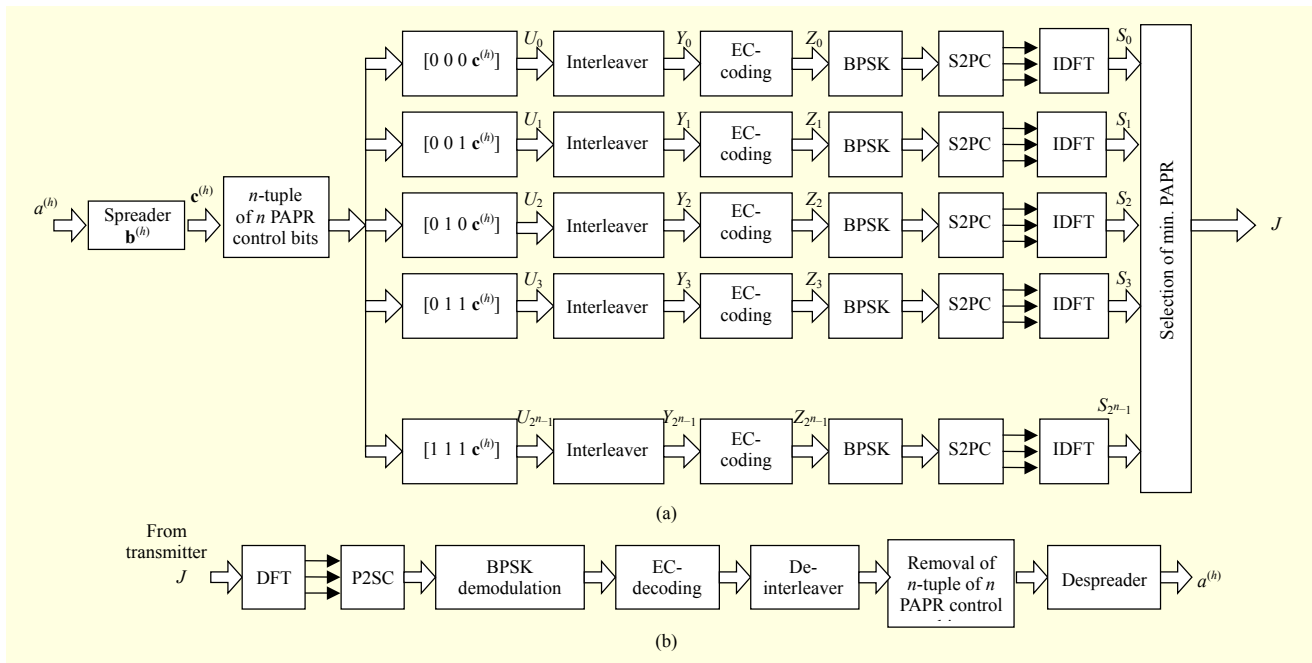
Fig. 3. (a) Block diagram of transmitter in an MC-CDMA system using NTSLM method and (b) block diagram of receiver in an MC-CDMA system using NTSLM method.

coding is represented as $\mathbf{Z} = [Z_0, Z_1, \dots, Z_{2^n-1}]$.

After error-control coding, the $\mathbf{Z}$ sequences are modulated using binary phase-shift keying followed by S2PC. After that, the $\mathbf{Z}$ sequences are fetched to an IDFT of size N_{IDFT}. The output from the IDFT is represented as $\mathbf{S} = [S_0, S_1, \dots, S_{2^n-1}]$. After the IDFT, the $\mathbf{S}$ time-domain sequences are checked to select a time-domain signal having the lowest PAPR for the transmission, J.

A block diagram of the MC-CDMA receiver using the NTSLM method is shown in Fig. 3(b). The selected time-domain signal J is received, as shown in Fig. 3(b). Upon receiving the selected time-domain signal J, it is subjected to a DFT of size N_{DFT}. The output from the DFT is a matrix of size $N_{\text{DFT}} \times 1$, which then goes to a parallel to serial converter, where it is then followed by a BPSK demodulation. After demodulation, the received signal is sent to error-control decoding prior to deinterleaving. To deinterleave a received signal, the receiver only needs to know which of the interleavers used at the transmitter has the lowest PAPR. After deinterleaving, the n-tuple of n PAPR control bits is removed prior to use of the signal despreader. Finally, user payload, $a^{(h)}$, is received and then transmitted.

1. ECCs

The ECCs inherent error detection and correction abilities make them a desirable option for persons seeking to reduce the PAPR in MC transmission systems [11]. An MC-CDMA

baseband signal is the sum of many data symbols modulated onto subcarriers. When the samples from all subcarriers are added in phase, the peak power of the signal becomes N times that of the average power; thus, this results in high PAPR. The key idea of using ECCs to reduce PAPR is to reduce the probability of subcarriers being added in phase. In this paper, Hamming, Golay, and convolutional codes are used as ECCs. These are described briefly in what follows.

A. Hamming Codes

Hamming code was an important ECC discovered by Richard Hamming in 1950 and is used for the error correction of faulty memory entries [22]. Hamming code is the best-known linear code. Its parameters are presented in Table 1 (for $m \geq 3$) [23].

Hamming code is defined by a parity-check matrix [23]. In this paper, a ($p = 7$, $k = 4$) Hamming code is used, which means $m = 3$ parity-check symbols are attached to an information of length k. The columns of the parity-check matrix for (7, 4) Hamming code comprise all nonzero 3-tuples. Since there are seven binary column vectors of length three, the parity-check matrix is of size 3×7.

$$H = \begin{bmatrix} 1 & 0 & 1 & 0 & 1 & 0 & 1 \\ 0 & 1 & 1 & 0 & 0 & 1 & 1 \\ 0 & 0 & 0 & 1 & 1 & 1 & 1 \end{bmatrix}. \quad (7)$$

By applying row operations to (7), a systematic parity-check

Table 1. Parameters of Hamming code.

Parameters	Value
Code length	$p = 2^m - 1$
Number of message bits	$k = 2^m - m - 1$
Number of parity bits	$p - k = m$

matrix of the binary Hamming code can be obtained [23]–[24].

$$H = \begin{bmatrix} I_3 \mid Q \end{bmatrix}, \quad (8)$$

$$H = \begin{bmatrix} 1 & 0 & 0 & 1 & 0 & 1 & 1 \\ 0 & 1 & 0 & 1 & 1 & 1 & 0 \\ 0 & 0 & 1 & 0 & 1 & 1 & 1 \end{bmatrix}. \quad (9)$$

The corresponding 4×7 generator matrix, G, is given as

$$G = [Q^T \mid I_4], \quad (10)$$

$$G = \begin{bmatrix} 1 & 1 & 0 & 1 & 0 & 0 & 0 \\ 0 & 1 & 1 & 0 & 1 & 0 & 0 \\ 1 & 1 & 1 & 0 & 0 & 1 & 0 \\ 1 & 0 & 1 & 0 & 0 & 0 & 1 \end{bmatrix}. \quad (11)$$

The parity-check matrix H, of (7, 4) binary Hamming code given in (9), has three columns that sum to equal the zero vector. Therefore, the minimum Hamming distance for a binary hamming code is $d_{\min} = 3$. The error-correcting ability, t, and error-detection capability, e, in terms of $d_{\min}$, are given respectively as

$$t = \left\lfloor \frac{d_{\min} - 1}{2} \right\rfloor = \lfloor 1 \rfloor \quad (12)$$

and

$$e = d_{\min} - 1 = 2, \quad (13)$$

where $\lfloor \ \rfloor$ is the floor function. A Hamming code is decoded using syndrome decoding [24].

B. Golay Codes

The (23, 12) Golay code, a cyclic code, was first learned by Golay in 1949 [25]. The (23, 12) Golay code is a perfect code with a minimum Hamming distance of 7 and so can correct three bit errors [23]–[24]. This paper uses a systematic (23, 12) cyclic Golay code.

Cyclic code is a sub-class of linear block code, which is easy to encode and decode. Any cyclically-shifted version of a cyclic codeword is also another codeword. If $U = (u_0, u_1, \dots, u_{p-1})$ is a codeword, then an end-round cyclic shift,

$U^{(1)} = (u_{p-1}, u_1, \dots, u_{p-2})$, is also certainly a codeword. In general, $U^{(i)} = (u_{p-i}, u_{p-i+1}, \dots, u_{p-1}, u_0, u_1, \dots, u_{p-i-1})$, obtained by the ith end-around cyclic shift, is a codeword. It is convenient to represent the cyclic codeword by a polynomial whose coefficients are equal to the components of the codeword; that is, as $U(X) = (u_0 + u_1 X + \cdots + u_{p-1} X^{p-1})$ [24]. An (p, k) cyclic code is best described by a generator polynomial $g(X) = (1 + g_1 X + g_2 X^2 + \cdots + g_p X^{p-k})$. Every codeword polynomial $U(X)$ is a multiple of $g(X)$ and can be represented as $U(X) = m(X)g(X)$, where $m(X) = (m_0 + m_1 X + m_2 X^2 + \cdots + m_{k-1} X^{p-k})$ is a message polynomial. An (p, k) cyclic code generator polynomial $g(X)$ must be of degree $(p - k)$, and a factor of $X^p + 1$; that is, $X^p + 1 = g(X)h(X)$, where $h(X)$ is a parity-check polynomial, which generates a $(p, p - k)$ cyclic code and must be of degree $p - (p - k)$ [23]. The generator polynomial $g(X)$ of (23, 12) Golay code is

$$g(X) = 1 + X + X^5 + X^6 + X^7 + X^9 + X^{11}. \quad (14)$$

The generator polynomial forms a 12×23 generator matrix, G, which is given as

$$G = \begin{bmatrix} 1 & 1 & 0 & 0 & 0 & 1 & 1 & 1 & 0 & 1 & 0 & 1 & 0 & 0 & 0 & 0 & 0 & 0 & 0 & 0 & 0 & 0 & 0 \\ 0 & 1 & 1 & 0 & 0 & 0 & 1 & 1 & 1 & 0 & 1 & 0 & 1 & 0 & 0 & 0 & 0 & 0 & 0 & 0 & 0 & 0 & 0 \\ 0 & 0 & 1 & 1 & 0 & 0 & 0 & 1 & 1 & 1 & 0 & 1 & 0 & 1 & 0 & 0 & 0 & 0 & 0 & 0 & 0 & 0 & 0 \\ 0 & 0 & 0 & 1 & 1 & 0 & 0 & 0 & 1 & 1 & 1 & 0 & 1 & 0 & 1 & 0 & 0 & 0 & 0 & 0 & 0 & 0 & 0 \\ 0 & 0 & 0 & 0 & 1 & 1 & 0 & 0 & 0 & 1 & 1 & 1 & 0 & 1 & 0 & 1 & 0 & 0 & 0 & 0 & 0 & 0 & 0 \\ 0 & 0 & 0 & 0 & 0 & 1 & 1 & 0 & 0 & 0 & 1 & 1 & 1 & 0 & 1 & 0 & 1 & 0 & 0 & 0 & 0 & 0 & 0 \\ 0 & 0 & 0 & 0 & 0 & 0 & 1 & 1 & 0 & 0 & 0 & 1 & 1 & 1 & 0 & 1 & 0 & 1 & 0 & 0 & 0 & 0 & 0 \\ 0 & 0 & 0 & 0 & 0 & 0 & 0 & 1 & 1 & 0 & 0 & 0 & 1 & 1 & 1 & 0 & 1 & 0 & 1 & 0 & 0 & 0 & 0 \\ 0 & 0 & 0 & 0 & 0 & 0 & 0 & 0 & 1 & 1 & 0 & 0 & 0 & 1 & 1 & 1 & 0 & 1 & 0 & 1 & 0 & 0 & 0 \\ 0 & 0 & 0 & 0 & 0 & 0 & 0 & 0 & 0 & 1 & 1 & 0 & 0 & 0 & 1 & 1 & 1 & 0 & 1 & 0 & 1 & 0 & 0 \\ 0 & 0 & 0 & 0 & 0 & 0 & 0 & 0 & 0 & 0 & 1 & 1 & 0 & 0 & 0 & 1 & 1 & 1 & 0 & 1 & 0 & 1 & 0 \\ 0 & 0 & 0 & 0 & 0 & 0 & 0 & 0 & 0 & 0 & 0 & 1 & 1 & 0 & 0 & 0 & 1 & 1 & 1 & 0 & 1 & 0 & 1 \end{bmatrix}. \quad (15)$$

The systematic generator matrix G_s of (15) is obtained by applying row operations on (15).

$$G_s = \begin{bmatrix} 1 & 0 & 1 & 0 & 1 & 1 & 1 & 0 & 0 & 0 & 1 & 1 & 0 & 0 & 0 & 0 & 0 & 0 & 0 & 0 & 0 & 0 & 0 \\ 1 & 1 & 1 & 1 & 1 & 0 & 0 & 1 & 0 & 0 & 1 & 0 & 1 & 0 & 0 & 0 & 0 & 0 & 0 & 0 & 0 & 0 & 0 \\ 1 & 1 & 0 & 1 & 0 & 0 & 1 & 0 & 1 & 0 & 1 & 0 & 0 & 1 & 0 & 0 & 0 & 0 & 0 & 0 & 0 & 0 & 0 \\ 1 & 1 & 0 & 0 & 0 & 1 & 1 & 1 & 0 & 1 & 1 & 0 & 0 & 0 & 1 & 0 & 0 & 0 & 0 & 0 & 0 & 0 & 0 \\ 1 & 1 & 0 & 0 & 1 & 1 & 0 & 1 & 1 & 0 & 0 & 0 & 0 & 0 & 0 & 1 & 0 & 0 & 0 & 0 & 0 & 0 & 0 \\ 0 & 1 & 1 & 0 & 0 & 1 & 1 & 0 & 1 & 1 & 0 & 0 & 0 & 0 & 0 & 0 & 1 & 0 & 0 & 0 & 0 & 0 & 0 \\ 0 & 0 & 1 & 1 & 0 & 0 & 1 & 1 & 0 & 1 & 1 & 0 & 0 & 0 & 0 & 0 & 0 & 1 & 0 & 0 & 0 & 0 & 0 \\ 1 & 0 & 1 & 1 & 0 & 1 & 1 & 1 & 1 & 0 & 0 & 0 & 0 & 0 & 0 & 0 & 0 & 0 & 1 & 0 & 0 & 0 & 0 \\ 0 & 1 & 0 & 1 & 1 & 0 & 1 & 1 & 1 & 1 & 0 & 0 & 0 & 0 & 0 & 0 & 0 & 0 & 0 & 1 & 0 & 0 & 0 \\ 0 & 0 & 1 & 0 & 1 & 1 & 0 & 1 & 1 & 1 & 1 & 0 & 0 & 0 & 0 & 0 & 0 & 0 & 0 & 0 & 1 & 0 & 0 \\ 1 & 0 & 1 & 1 & 1 & 0 & 0 & 0 & 1 & 1 & 0 & 0 & 0 & 0 & 0 & 0 & 0 & 0 & 0 & 0 & 0 & 1 & 0 \\ 0 & 1 & 0 & 1 & 1 & 1 & 0 & 0 & 0 & 1 & 1 & 0 & 0 & 0 & 0 & 0 & 0 & 0 & 0 & 0 & 0 & 0 & 1 \end{bmatrix}, \quad (16)$$

$$G_s = [Q \mid I_k].$$

The parity-check polynomial of (23, 12) Golay code is

$$h(X) = 1 + X + X^2 + X^3 + X^4 + X^7 + X^{10} + X^{12}. \quad (17)$$

The systematic parity-check matrix, H_s, is given by

$$H_s = [I_k \,|\, Q^T], \qquad (18)$$

$$H_s = \begin{bmatrix}
1 & 0 & 0 & 0 & 0 & 0 & 0 & 0 & 0 & 0 & 0 & 1 & 1 & 1 & 1 & 1 & 0 & 0 & 1 & 0 & 0 & 1 & 0 \\
0 & 1 & 0 & 0 & 0 & 0 & 0 & 0 & 0 & 0 & 0 & 1 & 1 & 1 & 1 & 1 & 0 & 0 & 1 & 0 & 0 & 1 \\
0 & 0 & 1 & 0 & 0 & 0 & 0 & 0 & 0 & 0 & 0 & 1 & 1 & 0 & 0 & 0 & 1 & 1 & 1 & 0 & 1 & 1 & 0 \\
0 & 0 & 0 & 1 & 0 & 0 & 0 & 0 & 0 & 0 & 0 & 1 & 1 & 0 & 0 & 0 & 1 & 1 & 1 & 0 & 1 & 1 & 1 \\
0 & 0 & 0 & 0 & 1 & 0 & 0 & 0 & 0 & 0 & 0 & 1 & 1 & 0 & 0 & 1 & 0 & 0 & 0 & 1 & 1 & 1 & 1 \\
0 & 0 & 0 & 0 & 0 & 1 & 0 & 0 & 0 & 0 & 0 & 1 & 0 & 0 & 1 & 1 & 1 & 0 & 1 & 0 & 1 & 0 & 1 \\
0 & 0 & 0 & 0 & 0 & 0 & 1 & 0 & 0 & 0 & 0 & 1 & 0 & 1 & 1 & 0 & 1 & 1 & 1 & 1 & 0 & 0 & 0 \\
0 & 0 & 0 & 0 & 0 & 0 & 0 & 1 & 0 & 0 & 0 & 1 & 0 & 1 & 1 & 0 & 1 & 1 & 1 & 1 & 1 & 0 & 0 \\
0 & 0 & 0 & 0 & 0 & 0 & 0 & 0 & 1 & 0 & 0 & 0 & 1 & 0 & 1 & 1 & 0 & 1 & 1 & 1 & 1 & 1 & 0 \\
0 & 0 & 0 & 0 & 0 & 0 & 0 & 0 & 0 & 1 & 0 & 0 & 0 & 1 & 0 & 1 & 1 & 0 & 1 & 1 & 1 & 1 & 1 \\
0 & 0 & 0 & 0 & 0 & 0 & 0 & 0 & 0 & 0 & 1 & 1 & 1 & 1 & 1 & 0 & 0 & 1 & 0 & 0 & 1 & 0 & 1
\end{bmatrix}.$$

$$(19)$$

C. Convolutional Codes

Binary convolutional code was created by Peter Elias in 1954 [26]. It is a special class of ECC in that the encoding can be viewed as a filtering or convolution operation. A convolutional encoder is not a memoryless device, unlike a block encoder [23]. A convolutional encoder is explained by the parameters in Table 2.

In Table 2, the constraint length K is defined as the number of bits stored in the shift registers plus a current input bit. In a convolutional encoder, p output bits at any given time depends not only on the k input bits at that time but also the inputs of $K - 1$ previous input bits [23].

This paper uses a nonsystematic feedforward convolutional encoder, shown in Fig. 4, due to its large free distance (d_{free}) and better performance with Viterbi decoding compared to systematic convolutional encoders [27]. The constraint length of this encoder is $K = 7$, as there are six shift registers plus a current input bit, and the code rate is 1/2. The generator polynomial of this encoder is a $k \times p$ matrix in octal and can be determined as follows, from the encoder shown in Fig. 4.

The first output bit is the modulo-2 sum of 1111001_2; that is, 171_8 in octal. The second output bit is the modulo-2 sum of 1011011_2; that is, 133_8 in octal. Therefore, the generator polynomial is $[171\ 133]_8$.

2. Computational Complexity

The computational complexity is one of the main factors to demonstrate the performance of a PAPR reduction scheme. Normally, the PAPR reduction capability of more complex techniques with less undesirable effects is better than the simple ones [28]. The computational complexity of the NTSLM method is certainly larger than that of the conventional SLM as it utilizes an interleaver and an ECC to reduce PAPR. Table 3 shows a comparison of the computational complexities between NTSLM and SLM.

To implement Q phase sequences in SLM, each of length N,

Table 2. Parameters of convolutional encoder.

Parameters	Value
Output bits at a time	p
Input bits at a time	k
Constraint length	K
Code rate	$R = k / p$

Table 3. Comparison of computational complexity between NTSLM and SLM.

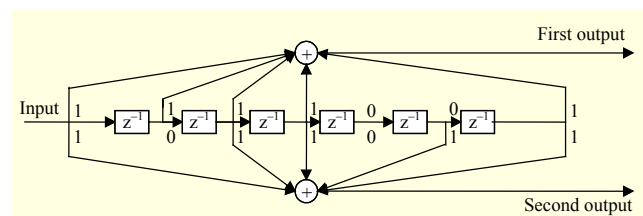| Method	Computational complexity
SLM	$2QN(1 + \log_2 N) + Q$ multiplications $3QN(1 + \log_2 N) + Q(N - 1) - 1$ additions
NTSLM	1. Hamming code $2QN$ modulo-2 additions $2QN(1 + \log_2 N) + Q$ multiplications $3QN(1 + \log_2 N) - Q - 1$ additions 2. Golay code $7QN$ modulo-2 additions $2QN(1 + \log_2 N) + Q$ multiplications $3QN(1 + \log_2 N) - Q - 1$ additions 3. Convolutional code $5QN$ modulo-2 additions $2QN(1 + \log_2 N) + Q$ multiplications $3QN(1 + \log_2 N) - Q - 1$ additions

Fig. 4. $[171\ 133]_8$ nonsystematic feedforward convolutional encoder.

QN additions are required to apply the phase sequences. After that, Q IFFT blocks are required, adding $2QN\log_2 N$ real multiplications and $3QN\log_2 N$ real additions. PAPRs for the Q permutations of the MC-CDAM signal are computed by $Q(2N + 1)$ real multiplications and $Q(3N - 2)$ real additions. Finally, $(Q - 1)$ subtractions or additions are necessary to find the minimum PAPR. The total complexity is $2QN(1 + \log_2 N) + Q$ real multiplications and $3QN(1 + \log_2 N) + Q(N - 1) - 1$ real additions [11].

For the computational complexity of the NTSLM method, the computational complexity of the interleaver is omitted. If $U = 2^n = Q$, then to implement a (7, 4) Hamming code, a (23, 12) Golay code, and a convolutional code, $2QN$, $7QN$, and $5QN$

modulo-2 additions are required, respectively. In addition, each code requires $2QN(1 + \log_2 N) + Q$ real multiplications and $3QN(1 + \log_2 N) - Q - 1$ real additions.

V. Simulation and Result Discussion

To verify the effectiveness of the proposed method, computer simulations are undertaken using MATLAB. The performance has been evaluated and compared by plotting the PAPR against the CCDF of the PAPR. The PAPR value at CCDF of 0.01% is used for comparison. The PAPR reduction performance is measured using the simulation parameters given in Table 4.

The PAPR performance comparison of Hamming, Golay, and convolutional codes in the NTSLM method with conventional SLM has been plotted for MC-CDMA in Fig. 5. The CCDF plot of Fig. 5 is plotted with $n = 6$ ($U = 2^6 = 64$) PAPR control bits for the NTSLM method and $Q = 64$ random phase sequences for conventional SLM. The x-axis represents the PAPR, and the y-axis represents the CCDF of the PAPR. A significant PAPR reduction achieved by the NTSLM method is evident from Fig. 5; that is, 5 dB, 8 dB, and 10 dB reductions using Hamming, Golay, and convolutional codes, respectively. It can also be deduced from Fig. 5 that the convolutional code is the best among the three ECCs used in the NTSLM method. Thus, it can be inferred from the results of Fig. 5 that the NTSLM method is effective in reducing the PAPR significantly compared to conventional SLM. Furthermore, unlike for SLM, the NTSLM method does not need any side information to recover the original data.

The CCDF plots of the PAPR of the MC-CDMA signals in Figs. 6, 7, and 8 compare the PAPR performance of the NTSLM with SLM for $n = 2, 3, \dots, 7$ ($U = 4, 8, \dots, 128$) PAPR control bits and their corresponding $Q = 4, 8, \dots, 128$ random phase sequences. It is evident from these CCDF plots that as the number of PAPR control bits increases, the PAPR reduction also increases. It can also be observed from these
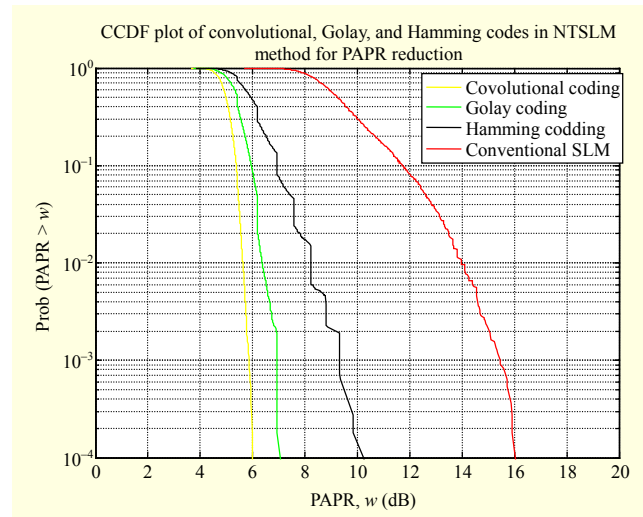

Fig. 5. CCDF of the PAPR of the MC-CDMA signals, comparing Hamming, Golay, and convolutional codes with conventional SLM for $U = 64$ and $Q = 64$.
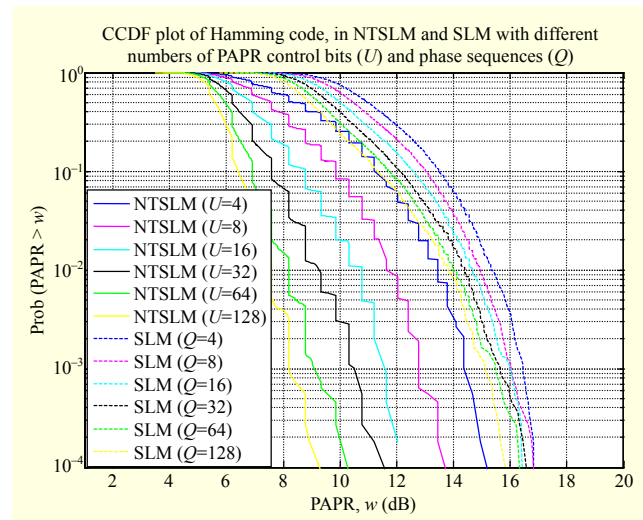

Fig. 6. CCDF of the PAPR of MC-CDMA signals compares a (7, 4) systematic Hamming code in NTSLM for $U = 4, 8, \dots, 128$ with conventional SLM for $Q = 4, 8, \dots, 128$.

figures that even with the least number of PAPR control bits in the NTSLM method, PAPR reductions of 2 dB, 4 dB, and 7.5 dB are achieved compared to conventional SLM. Therefore, it can be inferred that different numbers of PAPR control bits can be used to achieve a desired target PAPR reduction. Furthermore, it can also be deduced that the NTSLM method is a versatile one for PAPR reduction in an MC-CDMA signal.

The shapes of the performance curves of the NTSLM method are jagged compared to the shape of those for the conventional SLM method in Figs. 5, 6, and 7. This difference in shape is due to the use of block codes as ECCs in the NTSLM method. In the SLM method, the data, of length ℓ,

Table 4. Simulation parameters.

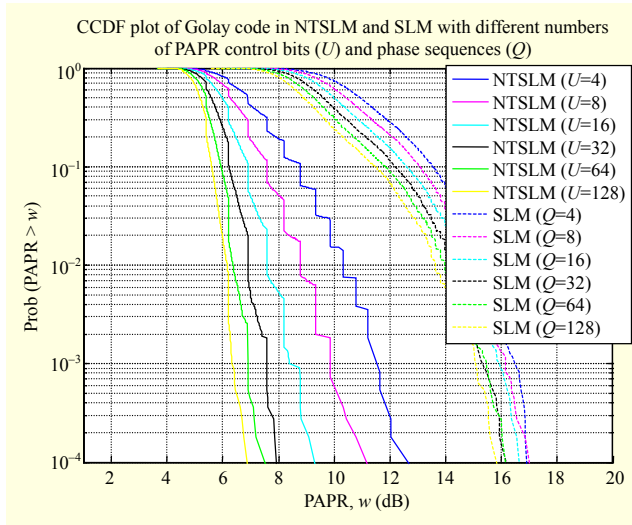| Parameters	Value
Number of subcarriers	128
Spreading sequence	Walsh–Hadamard
Spreading factor	8
Number of PAPR control bits	$2, 3, \dots, 7$
Hamming code primitive polynomial	$1 + x + x^3$
Convolutional code generator polynomial	$[171\ 133]_8$
Convolutional code constraint length	7

Fig. 7. CCDF of the PAPR of MC-CDMA signals compares a (23, 12) Golay code in NTSLM for $U = 4, 8, \ldots, 128$ with conventional SLM for $Q = 4, 8, \ldots, 128$.
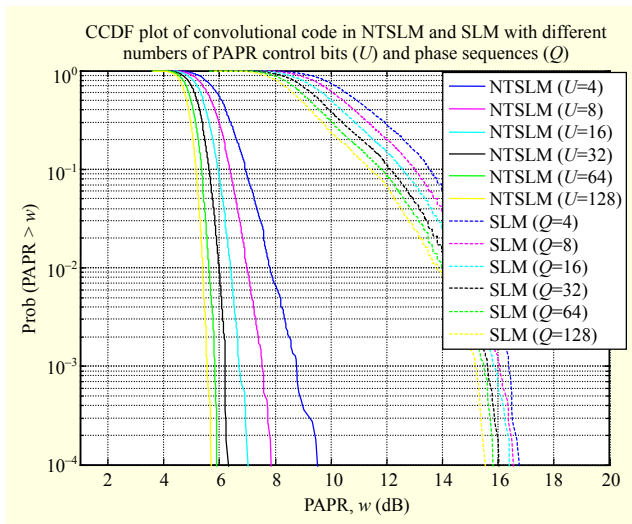

Fig. 8. CCDF of the PAPR of MC-CDMA signals compares a $[171 \ 133]_8$ nonsystematic feedforward convolutional code in NTSLM for $U = 4, 8, \ldots, 128$ with conventional SLM for $Q = 4, 8, \ldots, 128$.

is multiplied element-wise by statistically independent sequences of length ℓ. So, the binary combinations of the input or output in the SLM method are 2^ℓ. However, the Hamming and Golay codes are block codes and encode the data of length ℓ by taking 4 and 12 bits at a time, respectively. So, the maximum input or output binary combinations in the Hamming and Golay codes are 16 and 4,096, respectively. Further, it can be seen in Figs. 5, 6, and 7 that the Golay code performance curves are less jagged than those for the Hamming codes, due to the large block-code size of the Golay code compared to the Hamming code.

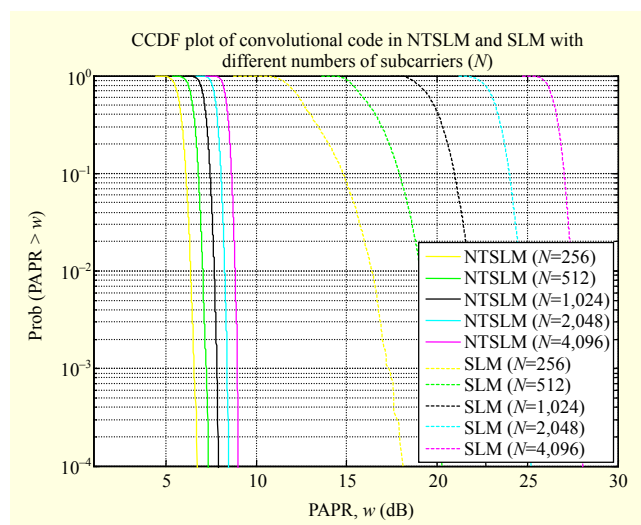The CCDF plots of the PAPR of the MC-CDMA signals in

Fig. 9. CCDF of the PAPR of MC-CDMA signal compares a $[171 \ 133]_8$ nonsystematic feedforward convolutional code in NTSLM with conventional SLM for $N = 256$, $512, \ldots, 4,096$.

Fig. 9 compare the PAPR performance of the NTSLM with SLM for $N = 256, 512, \ldots, 4,096$ subcarriers. It is evident from Fig. 9 that even with 4,096 subcarriers, the PAPR value is less than 10 dB using convolutional code in the NTSLM method. This shows the effectiveness of the NTSLM method in reducing the PAPR in the cases of large numbers of subcarriers.

VI. Conclusion

An improved SLM method for the reduction of PAPR in an MC-CDMA system is presented. The proposed method uses n-tuple of n PAPR control bits to generate 2^n sequences of an original data sequence. Each sequence is processed through an interleaver and ECC to improve the PAPR performance. The NTSLM method achieves a significant PAPR reduction without requiring the explicit side information to recover the original payload. Simulation results verify the effectiveness and versatility of the NTSLM method and also reveal that convolutional code provides maximum PAPR reduction for the MC-CDMA system compared to Golay and Hamming codes. A tradeoff between the number of n PAPR control bits and PAPR reduction can be observed from the simulation results. Thus, a large selection set size provides a significant PAPR reduction but with the disadvantage of having to have a higher number of IDFT operations compared to conventional SLM.

References

[1] K. Fazel and S. Kaiser, "*Multi-carrier and Spread Spectrum*

Systems: From OFDM and MC-CDMA to LTE and WiMAX," Chichester, UK: Wiley, 2008, pp. 46–56.

[2] L.A.P. Hernández and M.G. Otero, "User Reservation Approach for Peak-to-Average Power Ratio Reduction in MC-CDMA Systems," *IEEE Veh. Technol. Conf.*, Barcelona, Spain, Apr. 26–29, 2009, pp. 1–5.

[3] T. Jiang, C. Li, and C. Ni, "Effect of PAPR Reduction on Spectrum and Energy Efficiencies in OFDM Systems with Class: An HPA over AWGN Channel," *IEEE Trans. Broadcast.*, vol. 59, no. 3, Apr. 2013, pp. 513–519.

[4] J. Xia et al., "A Suboptimal TR Algorithm with Fixed Phase Rotation for PAPR Reduction in MC-CDMA System," *IET Int. Conf. Inf. Commun. Technol.*, Beijing, China, Apr. 27–29, 2013, pp. 415–420.

[5] Y. Wang et al., "Nonlinear Companding Transform for Reduction of Peak to Average Power OFDM Systems," *IEEE Trans. Broadcast.*, vol. 59, no. 2, Oct. 2012, pp. 369–375.

[6] F. Giannetti, V. Lottici, and I. Stupia, "PAPR Analytical Characterization and Reduced-PAPR Code Allocation Strategy for MC-CDMA Transmissions," *IEEE Trans. Wireless Commun.*, vol. 10, no. 1, Dec. 2010, pp. 219–227.

[7] M.C. Paredes and M.J. Fernández-Getino García, "Energy Efficient Peak Power Reduction in OFDM with Amplitude Pre-distortion Aided by Orthogonal Pilots," *IEEE Trans. Consum. Electron.*, vol. 59, no. 1, Feb. 2013, pp. 45–53.

[8] J. Ji and G. Ren, "A New Modified SLM Scheme for Wireless OFDM Systems without Side Information," *IEEE Signal Process. Lett.*, vol. 20, no. 11, Aug. 2013, pp. 1090–1093.

[9] S. Khademi and A.V.D. Veen, "Constant Modulus Algorithm for Peak-to-Average Power Ratio (PAPR) Reduction in MIMO OFDM/A," *IEEE Signal Process. Lett.*, vol. 20, no. 5, May 2013, pp. 531–534.

[10] P. Kryszkiewicz and H. Bogucka, "Out-of-Band Power Reduction in NC-OFDM with Optimized Cancellation Carriers Selection," *IEEE Commun. Lett.*, vol. 17, no. 10, Aug. 2013, pp. 1901–1904.

[11] Y. Rahmatallah and S. Mohan, "Peak-to-Average Power Ratio Reduction in OFDM Systems: A Survey and Taxonomy," *IEEE Commun. Surveys Tutorials*, vol. 15, no. 4, Mar. 2013, pp. 1567–1592.

[12] X. Li and L.J. Cimini, "Effects of Clipping and Filtering on the Performance of OFDM," *IEEE Commun. Lett.*, vol. 2, no. 5, May 1998, pp. 131–133.

[13] S.H. Muller and J.B. Huber, "OFDM with Reduced Peak-to-Average Power Ratio by Optimum Combination of Partial Transmit Sequences," *Electron. Lett.*, vol. 33, no. 5, Feb. 1997, pp. 368–369.

[14] R.W. Bauml, R.F.H. Fischer, and J.B. Huber, "Reducing the Peak-to-Average Power Ratio of Multi-carrier Modulation by Selected Mapping," *Electron. Lett.*, vol. 32, no. 22, Oct. 1996, pp. 2056–2057.

[15] M. Breiling, S.H. Muller-Weinfurtner, and J.B. Huber, "SLM Peak-Power Reduction without Explicit Side Information," *IEEE Commun. Lett.*, vol. 5, no. 6, June 2001, pp. 239–241.

[16] N. Ruangsurat and R.M.A.P. Rajatheva, "An Investigation of Peak-to-Average Power Ratio in MC-CDMA Combined with Partial Transmit Sequence," *IEEE Veh. Technol. Conf.*, Rhodes, VA, USA, vol. 1, May 6–9, 2001, pp. 761–765.

[17] N. Ohkubo and T. Ohtsuki, "A Peak to Average Power Ratio Reduction of Multi-carrier CDMA Using Selected Mapping," *IEEE Veh. Technol. Conf.*, Vancouver, Canada, vol. 4, Sept. 24–28, 2002, pp. 2086–2090.

[18] S. Ruangsuthinarupap et al., "PAPR Reduction by Combining Selected Mapping and Selected Spreading Code in MC-CDMA Systems," *IEEE Int. Symp. Comput. Commun.*, Alexandria, Egypt, vol. 2, June 28–July 1, 2004, pp. 725–729.

[19] J. Wang, J. Luo, and Y. Zhang, "A New Phase Sequence for SLM in MC-CDMA System," *Wireless Commun.*, *Netw. Mobile Comput. Conf.*, Shanghai, China, Sept. 21–25, 2007, pp. 938–941.

[20] N. Ohkubo and T. Ohtsuki, "Design Criteria for Phase Sequences in Selected Mapping," *IEEE Veh. Technol. Conf.*, Jeju, Rep. of Korea, Apr. 22–25, 2003, pp. 373–377.

[21] T. Jiang and Y. Wu, "An Overview: Peak-to-Average Power Ratio Reduction Techniques for OFDM Signals," *IEEE Trans. Broadcast.*, vol. 54, no. 2, June 2008, pp. 257–268.

[22] R.W. Hamming, "Error Detecting and Error Correcting Codes," *Bell Syst. Techn. J.*, vol. 29, no. 2, Apr. 1950, pp. 147–160.

[23] B. Sklar, "*Digital Communications: Fundamentals and Application*," Upper Saddle River, NJ, USA: Prentice Hall, 2001, pp. 366–429.

[24] A. Neubauer, J. Freudenberger, and V. Kuhn, "*Coding Theory Algorithms, Architectures and Applications*," Chichester, UK: Wiley, 2007, pp. 13–157.

[25] M.J.E. Golay, "Notes on Digital Coding," *Proc. IRE*, vol. 37, no. 8, Aug. 1949, p. 657.

[26] P. Elias, "Error-Free Coding," *Trans. IRE Professional Group Inf. Theory*, vol. 4, no. 4, Sept. 1954, pp. 29–37.

[27] P. Sweeney, "*Error Control Coding*," Chichester, UK: Wiley, 2002, pp. 35–64.

[28] S.H. Han and J.H. Lee, "An Overview of Peak-to-Average Power Ratio Reduction Techniques for Multi-carrier Transmission," *IEEE Wireless Commun.*, vol. 12, no. 2, Apr. 2005, pp. 56–65.

Sajjad Ali received his BE degree in telecommunication engineering and his ME degree in communication systems networks from Mehran University of Engineering & Technology (MUET), Jamshoro, Pakistan, in 2007 and 2011, respectively. He joined Telenor Pakistan as an operation and maintenance engineer in 2007. He then joined the Department of Telecommunication Engineering, MUET, as a lab lecturer in 2008 and became an assistant professor in 2011. He is currently pursuing his PhD degree at Dalian University of Technology, China. His research interests are in the field of digital signal processing and broadband wireless communications.

Zhe Chen received his BS degree in electronic engineering and his MS and PhD degrees in signal and information processing from Dalian University of Technology (DUT), China, in 1996, 1999, and 2003, respectively. He joined the Department of Electronic Engineering, DUT, as a lecture in 2002 and became an associate professor in 2006. His research interests include digital signal processing, speech processing, image processing, and broadband wireless communications.

Fuliang Yin received his BS degree in electronic engineering and his MS degree in communications and electronic systems from Dalian University of Technology (DUT), China, in 1984 and 1987, respectively. He joined the Department of Electronic Engineering, DUT, as a lecturer in 1987 and became an associate professor in 1991. He has been a professor at DUT since 1994 and the dean of the School of Electronic and Information Engineering of DUT from 2000 to 2009. His research interests include digital signal processing, speech processing, image processing, and broadband wireless communications.